The Plant Cell, Vol. 17, 3035–3050, November 2005, www.plantcell.org © 2005 American Society of Plant Biologists

Cell Cycle Progression in the Pericycle Is Not Sufficient for SOLITARY ROOT/IAA14-Mediated Lateral Root Initiation in *Arabidopsis thaliana* [W]

Steffen Vanneste,[a] Bert De Rybel,[a] Gerrit T.S. Beemster,[a] Karin Ljung,[b] Ive De Smet,[a] Gert Van Isterdael,[a] Mirande Naudts,[a] Ryusuke Iida,[c] Wilhelm Gruissem,[d] Masao Tasaka,[c] Dirk Inzé,[a] Hidehiro Fukaki,[c] and Tom Beeckman[a,1]

[a] Department of Plant Systems Biology, Flanders Interuniversity Institute for Biotechnology, Ghent University, B-9052 Ghent, Belgium

[b] Umeå Plant Science Center, Department of Forest Genetics and Plant Physiology, Swedish University of Agricultural Sciences, SE-901 83, Umeå, Sweden

[c] Graduate School of Biological Sciences, Nara Institute of Science and Technology, Ikoma 630-0101, Nara, Japan

[d] Institute of Plant Sciences, Swiss Federal Institute of Technology and Zurich-Basel Plant Science Center, CH-8092 Zürich, Switzerland

To study the mechanisms behind auxin-induced cell division, lateral root initiation was used as a model system. By means of microarray analysis, genome-wide transcriptional changes were monitored during the early steps of lateral root initiation. Inclusion of the dominant auxin signaling mutant *solitary root1* (*slr1*) identified genes involved in lateral root initiation that act downstream of the auxin/indole-3-acetic acid (AUX/IAA) signaling pathway. Interestingly, key components of the cell cycle machinery were strongly defective in *slr1*, suggesting a direct link between AUX/IAA signaling and core cell cycle regulation. However, induction of the cell cycle in the mutant background by overexpression of the D-type cyclin (*CYCD3;1*) was able to trigger complete rounds of cell division in the pericycle that did not result in lateral root formation. Therefore, lateral root initiation can only take place when cell cycle activation is accompanied by cell fate respecification of pericycle cells. The microarray data also yielded evidence for the existence of both negative and positive feedback mechanisms that regulate auxin homeostasis and signal transduction in the pericycle, thereby fine-tuning the process of lateral root initiation.

INTRODUCTION

Auxins have long been put forward as potent stimulators of cell division (Gautheret, 1939), but although considerable progress has been made in our understanding of both auxin signaling (Weijers and Jürgens, 2004) and cell cycle progression (Inzé, 2005), the molecular mechanisms by which these processes are connected remain poorly understood (Vanneste et al., 2005). The initiation of lateral roots, marked by specific cell divisions in the pericycle (Casimiro et al., 2001), is triggered by auxin (Torrey, 1950) and is, therefore, an ideal model system for studying how auxin signaling activates cell cycle progression.

The onset of lateral root formation coincides with the occurrence of a series of anticlinal, asymmetric divisions in the xylem pole pericycle (Malamy and Benfey, 1997); hence, cell cycle activation is inherently connected with lateral root initiation. Activation and progression through the major phases of the cell cycle (G1, S, G2, and M) are governed by the control of cyclin-dependent kinases (CDKs). The activity of these CDKs can be modulated through interacting regulatory components (cyclins [Roudier et al., 2000; Dewitte et al., 2003; Lee et al., 2003] and CDK subunits [De Veylder et al., 1997]), inhibitory components (inhibitors of CDKs and Kip-related proteins [Wang et al., 1997; De Veylder et al., 2001]), or through stimulatory (Shimotohno et al., 2004) and inhibitory phosphorylation (Sun et al., 1999). Beeckman et al. (2001) showed that in *Arabidopsis thaliana*, pericycle cells leaving the root apical meristem remain in G1 phase. Under normal conditions, only the pericycle cells at the xylem pole retain the capability to respond to an inductive signal, such as auxin, to initiate lateral roots. Interestingly, the expression of the cell cycle inhibitor KRP2 is strongly downregulated in xylem pole pericycle cells when roots are subjected to auxin treatment (Himanen et al., 2002; Casimiro et al., 2003). However, it can be anticipated that numerous regulatory proteins will be involved in lateral root initiation.

For global studies of developmental processes at the molecular level, relatively large quantities of material are required but are almost impossible to obtain for lateral root initiation because of the small subsets of pericycle cells involved (Laskowski et al.,

[1] To whom correspondence should be addressed. E-mail tom.beeckman@psb.ugent.be; fax 32-9-3313809.

The authors responsible for distribution of materials integral to the findings presented in this article in accordance with the policy described in the Instructions for Authors (www.plantcell.org) are: Hidehiro Fukaki (h-fukaki@bs.naist.jp) and Tom Beeckman (tom.beeckman@psb.ugent.be).

[W] Online version contains Web-only data.

Article, publication date, and citation information can be found at www.plantcell.org/cgi/doi/10.1105/tpc.105.035493.

1995; Kurup et al., 2005). Based on the observation that inhibition of polar auxin transport prevents lateral root initiation (Casimiro et al., 2001), a lateral root-inducible system (LRIS) was developed and characterized (Himanen et al., 2002, 2004). Germination on media with sufficiently high levels of 1-*N*-naphthylphthalamic acid (NPA) results in roots without lateral root initiation sites, which can be induced synchronously throughout the pericycle by subsequent transfer to media with high auxin concentrations (Himanen et al., 2002). This system allows the monitoring of the sequential signaling and cell cycle progression during lateral root initiation (Himanen et al., 2004).

Prior to inducing cell division, auxins have to be perceived and transmitted to turn on the cell cycle machinery. The current understanding of early auxin signal transduction is focused on the 26S proteasome-dependent proteolysis of specific small short-lived nuclear proteins, designated auxin/indole-3-acetic acid (AUX/IAA) (reviewed in Dharmasiri and Estelle, 2004). AUX/IAA proteins belong to a family of 29 members (Liscum and Reed, 2002) and act as negative regulators by repressing auxin response factors (ARFs) (Tiwari et al., 2004). When the auxin concentration increases, the interaction between the SCF^{TIR1} E3-ligase and AUX/IAA proteins is stimulated by direct binding of auxin to a family of auxin binding F-boxes (Dharmasiri et al., 2005a, 2005b; Kepinski and Leyser, 2005), resulting in oligoubiquitination of AUX/IAA proteins (Gray et al., 2001). Such ubiquitinated proteins are usually targeted for 26S proteasome-mediated proteolysis (Hershko and Ciechanover, 1998). Thus, high auxin concentration derepresses ARF activity, allowing the primary auxin response to take place. When AUX/IAA proteins are mutated in domain II, essential for the interaction with the SCF^{TIR1} complex (Ramos et al., 2001), their stability increases dramatically, resulting in auxin-resistant phenotypes (Ouellet et al., 2001; Zenser et al., 2001). Over the years, an increasing number of dominant and semidominant *aux/iaa* mutants have been described that exhibit point mutations in domain II (Liscum and Reed, 2002). When mutated in domain II, *solitary root1* (*slr1*) mutants develop a primary root without any sign of lateral root initiation (Fukaki et al., 2002). Therefore, the SLR/IAA14 protein is probably a central regulator of lateral root initiation.

Here, lateral root initiation was used as an in planta model to study the interaction between the auxin signaling pathway and cell cycle activation. For this purpose, the lateral rootless phenotype of the early auxin signaling mutant *slr1* was utilized to compare on a genome-wide level the transcriptional changes that occur in root segments of the wild type and *slr1* during auxin-induced lateral root initiation. Complementation by overexpression of *CYCD3;1* in the *slr1* pericycle was able to trigger cell divisions, but no lateral root initiation, suggesting that more is involved than the activation of cell cycle progression in the pericycle. The transcriptional data suggest that during lateral root initiation, counteracting feedback regulation acts on auxin homeostasis and the signal transduction machinery. Furthermore, the analysis of the transcriptional changes in the wild type versus the *slr1* mutant allowed some cell cycle regulators to be pinpointed as potential targets of the primary auxin signaling pathway.

RESULTS

slr1 as a Tool to Link Auxin Signaling to Lateral Root Initiation

The dominant mutation in *SLR/IAA14* results in complete absence of detectable lateral root initiation sites, formation of aberrant root hairs, and agravitropic root growth (Fukaki et al., 2002). For a better notion of the tissues and cell types that become the primary targets of the reduced auxin response in the mutant, we analyzed the expression pattern of *SLR/IAA14* at the cellular level by anatomical sections of 3-d-old roots of transgenic plants harboring a promoter IAA14/β-glucuronidase (P_{IAA14}:*GUS*) construct. Expression of mutant *slr/iaa14* under control of this promoter sequence has been shown to be sufficient to phenocopy the root phenotype of *slr1* (Fukaki et al., 2002). Furthermore, tissue-specific expression of stabilized SLR/IAA14 in the xylem pole pericycle conferred the lateral rootless phenotype of *slr1* (Fukaki et al., 2005). The expression of P_{IAA14}:*GUS* was strongest in the xylem pericycle cells, in the xylem-associated cells of mature root tissues, and almost absent from phloem pole pericycle cells (Figures 1A and 1B). This stronger expression at the xylem pole, the site of lateral root initiation in *Arabidopsis*, suggests a causal link between the reduced auxin responsiveness and the lack of lateral roots in the mutant. During lateral root development, GUS activity was strongest in the youngest lateral root primordia, whereas it was nearly absent in mature lateral root meristems (see Supplemental Figure 1 online). In epidermal cells of mature root tissues, the expression was also low (Figure 1A). In the elongation zone, expression was strongest in epidermal cells (Figure 1C), whereas more distally, it was restricted to the lateral root cap (Figure 1D). Plants harboring the P_{IAA14}:*GUS* construct were crossed into the *slr1* background, resulting in F1 plants exhibiting a reduced level of expression compared with that of the wild type (Figures 1E and 1F). Anatomical sections showed that the tissue specificity of P_{IAA14}:*GUS* expression was maintained in *slr1* (data not shown). When the primary root length was compared between 2-week-old wild-type and mutant seedlings, no significant differences were observed (data not shown), suggesting that the meristematic activity of the *slr1* primary roots was not affected. To verify whether *slr1* mutants still normally specified the pericycle, the enhancer trap line, J0121, a marker for xylem pericycle cell identity (Casimiro et al., 2001), was crossed into the *slr1* mutant. The green fluorescent protein expression pattern of J0121 did not change significantly when compared with the wild-type situation (Figures 1G and 1H). Because CDKA;1 is a central regulator of cell cycle progression and its expression is associated with competence to divide (Hemerly et al., 1993), the $P_{CDKA;1}$:*GUS* fusion was analyzed. Its expression was equally strong in the pericycle of the wild type and *slr1* (Figures 1I and 1J). Also, expression of P_{ALF4}:*GUS*, fused with ALF4, a protein with unknown function that is required for maintaining pericycle cells competent to form lateral roots (DiDonato et al., 2004), was unaltered in *slr1* (data not shown). These observations indicate that the changes in auxin response and cell cycle activation in the mutant are probably not due to an altered pericycle identity or a reduced competence to divide.

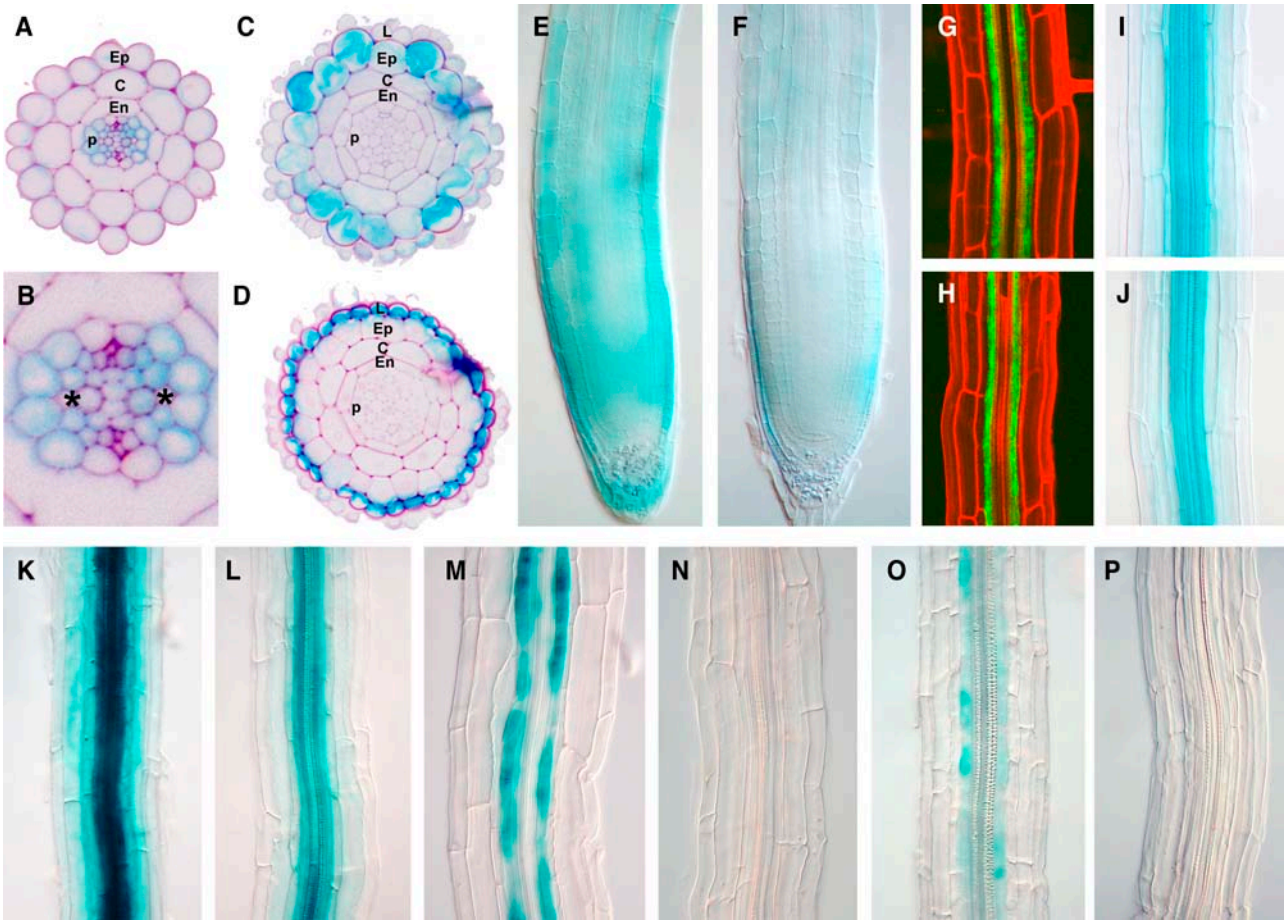

Figure 1. Expression Analysis in the Wild Type and *slr1*.

(A) to **(D)** Anatomical sections of P_{IAA14}:*GUS* mature root tissue **(A)**, detail of stele **(B)**, elongation zone **(C)**, and root meristem **(D)** in wild-type background.

(E) and **(F)** P_{IAA14}:*GUS* expression in root apical meristem in the wild type and in *slr1*, respectively.

(G) and **(H)** Xylem pole pericycle-specific green fluorescent protein expression in mature root segment of J0121 in the wild type and in *slr1*, respectively.

(I) and **(J)** $P_{CDKA;1}$:*GUS* expression in the wild type and in *slr1*, respectively.

(K) to **(P)** Expression in roots germinated on 10 μM NPA and transferred 72 h after germination to 10 μM NAA for 12 h of P_{DR5}:*GUS* expression in the wild type **(K)**, P_{DR5}:*GUS* expression in *slr1* **(L)**, $P_{CYCB1;1}$:*GUS* in the wild type **(M)**, $P_{CYCB1;1}$:*GUS* in *slr1* **(N)**, $P_{CDKB1;1}$:*GUS* in the wild type **(O)**, and $P_{CDKB1;1}$:*GUS* in *slr1* **(P)**.

C, cortex; En, endodermis; Ep, epidermis; L, lateral root cap; p, pericycle. Asterisk indicates protoxylem cells.

To compare the transcriptional changes associated with auxin induction in the wild-type and the *slr1* situations, we used the recently developed LRIS that allows the synchronization of lateral root initiation in roots devoid of lateral roots (Himanen et al., 2002). The possibility that this LRIS might induce lateral root initiation in the mutant was first addressed before initiating large-scale experiments. Therefore, specific GUS reporter lines were crossed into the mutant background, and their response to a 12-h auxin treatment following a 72-h growth on NPA was characterized. In 72-h NPA-treated seedlings, no expression of the auxin-responsive P_{DR5}:*GUS* construct could be detected in either genotype (data not shown). When seedlings had been transferred to α-naphthaleneacetic acid (NAA) for 12 h, P_{DR5}:*GUS* activity was strongly induced throughout the root in the wild type and to a lesser extent in *slr1* (Figures 1K and 1L), suggesting that the *slr1* mutation also results in reduced auxin responsiveness within the LRIS. To assay cell cycle progression within the LRIS, plants harboring GUS reporter constructs for the G2-to-M transition-associated genes *CYCB1;1* and *CDKB1;1* were used. The expression of *CYCB1;1* is strong in pericycle cells undergoing the first divisions of lateral root initiation (Beeckman et al., 2001; Himanen et al., 2002), whereas that of *CDKB1;1* starts from the S phase into the G2-to-M transition (Porceddu et al., 2001; Menges and Murray, 2002). With these two GUS reporter lines, no expression was detected in the pericycle in either genotype when germinated on NPA (data not shown). When transferred to auxin for 12 h, wild-type pericycle cells had very strong GUS activity for both markers, hinting that these

pericycle cells divide actively (Figures 1M and 1O). The destruction box fused to GUS in $P_{CYCB1;1}$:*GUS* results in proteolysis during the late mitosis. Therefore, because of its patchy GUS pattern, the GUS-stained pericycle cells might have undergone at least one cycle of cell division during the 12-h NAA treatment. On the other hand, no GUS activity could be induced in *slr1* pericycle cells (Figures 1N and 1P), reflecting the complete absence of mitotic activity, following 12 h of auxin treatment. These data legitimize the use of the *slr1* mutant in a genome-wide transcriptional analysis of lateral root initiation.

Microarray Setup and Statistical Analysis

Within the LRIS, pericycle cells have been shown to be blocked in the G1 phase when germinated on NPA (Himanen et al., 2002, 2004). Subsequent transfer to auxin media was sufficient to trigger the primary auxin response within 2 h, resulting in a synchronous induction of lateral root initiation over the entire pericycle (visualized by $P_{CYCB1;1}$:*GUS* expression in Figure 2). To gain insight into the early events of lateral root initiation, samples for microarray analysis were taken at the time points 0 h NAA (= 72 h NPA), 2 h NAA, and 6 h NAA for both the wild type and *slr1* (highlighted stages in Figure 2). Per time point, ~1000 root segments were sampled and two independent biological replicates were performed. To minimize contamination with nonrelevant tissues and dividing cells, root segments were cut above the root apical meristem and below the root-hypocotyl junction. These segments were further subjected to the required steps for microarray analysis with the ATH1 Affymetrix chips harboring 22,746 probe sets (see Methods). Analysis of variance on the normalized gene expression data assessed the significance of three major sources of variability affecting the expression level: the duration of the auxin treatment (time), the genotype, and the interaction between these two. Correction for multiple comparisons was performed by controlling the false discovery rate, and q-values were calculated according to Storey and Tibshirani (2003). At a stringency level of $P < 0.001$, 3110 genes had a significantly modulated expression profile during the experiment.

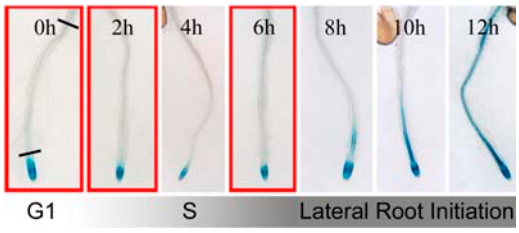

Figure 2. Schematic Representation of the LRIS.

Seeds are germinated on medium supplemented with NPA to inhibit lateral root initiation. The pericycle cells of seedlings germinated on NPA are in G1 phase (0 h). Subsequent transfer to NAA-supplemented medium induces gradual cell cycle progression over S, G2, and M phases, corresponding to synchronized lateral root initiation. $P_{CYCB1;1}$:*GUS* activity marks G2-to-M transition. Red rectangles indicate time points used for the microarray. The segment between root tip and root-hypocotyl junction (black lines at 0 h) was used for the microarray analysis.

Furthermore, none of them could be rejected based on the calculated q-values ($q < 0.05$) (see Supplemental Table 1 online).

Cross-Table Clustering to Identify Lateral Root Initiation Genes

The generally used approaches of hierarchical (Eisen et al., 1998) and K means (Tavazoie et al., 1999; Soukas et al., 2000) clustering allow the classification of gene expression patterns of single-series microarray time courses. However, for the comparison of multiple-series microarray time courses, no standard algorithms are established. Most reports on such issues restrict themselves to fold-change comparisons (Tian et al., 2002; Ullah et al., 2003) or basic diagrams (Puthoff et al., 2003; Taji et al., 2004). Less frequently, clustering is used to identify differences between expression profiles in different genotypes (De Paepe et al., 2004). Here, a new approach was developed based on the commonly used single-series time course K means clustering algorithm (Figure 3A). By combining the data irrespective of the genetic background (0, 2, and 6 h) with the K means clustering algorithm, the gene expression profiles could be classified into 14 clusters (Figure 3B). Subsequently, the clusters were plotted at the headings of rows and columns of a cross-table. In this cross-table format, the expression profile of each gene is summarized by a uniquely identifiable cluster combination corresponding to the expression pattern in the wild type and in *slr1*. Per cluster combination, the gene frequency was calculated and included into the cross-table; a color code was implemented to assess easily the differential dynamics of expression between both genotypes (Figure 3C; see Supplemental Table 1 online). Hereafter, we will refer to this methodology as cross-table clustering. This approach allows a high-resolution representation of gene expression patterns across multiple genotypes and provides a tool to compare the transcriptional changes in the wild type versus mutant within the framework of a unified set of expression profiles.

In order to gain further insight into the data set, the functional relevance of all types of cluster combinations was evaluated. The wild-type expression profiles were subdivided into three major patterns: upregulated (Figure 3B, clusters 1 to 6), constitutive (Figure 3B, clusters 7 to 11), and downregulated (Figure 3B, clusters 12 to 14). These expression patterns were compared with the corresponding expression profiles in *slr1*. The genes represented by cluster combinations on the diagonal of the cross-table (gray) exhibit expression profiles that are similar in both genotypes, whereas above (red and orange) and below (green and blue) the diagonal, the induction rates in the wild type are higher and lower than those in the mutant, respectively. The Gene Ontology classification for biological function (Berardini et al., 2004) was applied on all annotated genes of each subgroup and subsequently compared with all annotated significant genes within our experiment with the EASE 2.1 software (Hosack et al., 2003). The 913 genes that were upregulated dependent on wild-type SLR/IAA14 stability (selection in Figure 3C; see Supplemental Table 2 online) were significantly enriched ($P_{Bonferoni} < 0.01$) in proliferation-related biological functions, such as cell cycle, nucleic acid metabolism, and protein metabolism (Figure 4; see Supplemental Table 3A online), but restricting this

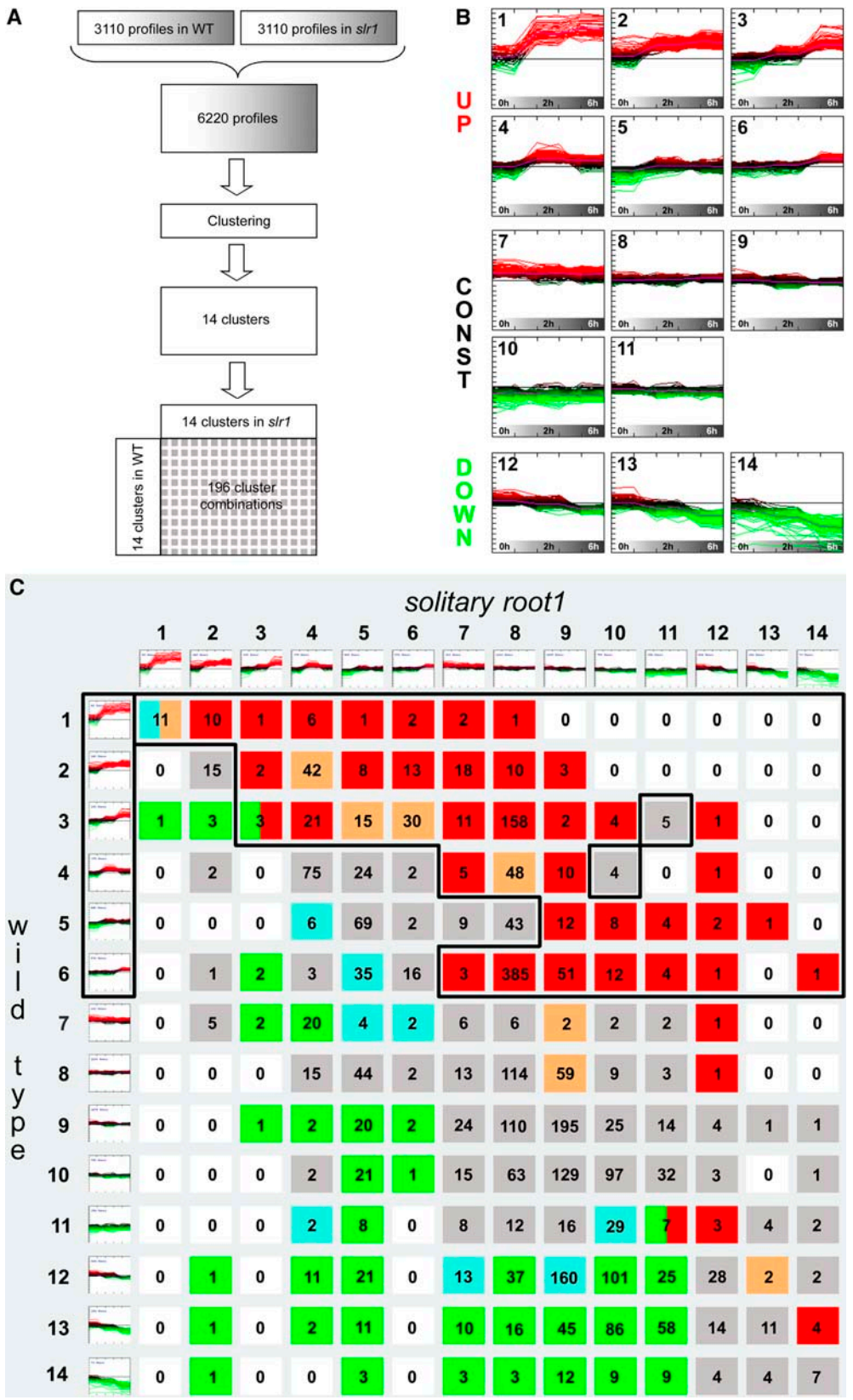

Figure 3. Cluster Analysis of the Expression Data.

selection to the earliest induced genes (Figure 3B, cluster 1 to 3) resulted in a significant enrichment ($P_{Bonferoni} < 0.01$) in the biological functions response to endogenous stimulus and response to auxin stimulus (see Supplemental Table 3B online). These observations strongly correlate with the previous observations of Himanen et al. (2004), who found that within the LRIS, genes related to signaling were upregulated early prior to cell cycle activation.

In conclusion, the cross-table clustering methodology on our data set reliably identified 913 genes that depend on rapid SLR/IAA14 degradation for normal auxin responsiveness. Because *slr1* does not initiate lateral roots, even upon auxin treatment, such genes might encode potential regulatory proteins required for lateral root initiation and will be designated as lateral root initiation (*LRI*) genes hereafter.

Validation of *LRI* Genes by Database Comparison

With the same LRIS, we had performed previously a microarray study based on cDNA microarrays representing ~4600 genes (Himanen et al., 2004). At a stringency level of 0.005, 906 genes had been found to be significantly expressed. The profiles of 343 genes were clustered into three upregulated clusters. From the selected 913 *LRI* genes, defined as auxin inducible in an SLR/IAA14-dependent manner, 122 genes were also represented in the earlier data set (see Supplemental Table 4 online). This result suggests that, despite the differences in type of array (cDNA array versus Affymetrix gene chip) and the differences in statistical analysis, a high level of reproducibility was obtained by the LRIS and implies also that a high level of confidence can be attributed to the profiles associated with the *LRI* genes, as suggested by the q-values.

The *arf7 arf19* double mutants have been shown to phenocopy the lateral rootless phenotype of *slr1* to a large extent (Okushima et al., 2005; Wilmoth et al., 2005), indicating that SLR/IAA14 inhibits the activity of these ARFs to block lateral root initiation. Recently, a yeast two-hybrid assay confirmed that SLR/IAA14 interacts with ARF7 and ARF19 (Fukaki et al., 2005). Therefore, both *slr1* and *arf7 arf19* mutants can be expected to have similar target genes. The auxin inducibility in *arf7 arf19* has been assessed by Okushima et al. (2005), who assayed the effects of a 2-h treatment with 5 μM IAA on 5-d-old seedlings of wild type, *arf7*, *arf19*, and *arf7 arf19* in a microarray that gave a robust overview of early auxin-induced genes. The respective ARF7- and ARF19-dependent auxin inducibility of the 913 *LRI* genes was extracted from the published data set (see Supplemental Table 5 online). Of the 913 *LRI* genes, 99 were induced more than twofold in the wild type, whereas the auxin inducibility of these genes was abolished in the *arf7 arf19* double mutants (see Supplemental Table 6 online). Because in this experimental setup only a 2-h IAA treatment was used, a large percentage of these genes belong to the early induced *LRI* genes (83 out of 365 genes in wild-type clusters 1 to 3). Due to large experimental differences, we cannot exclude that more *LRI* genes act downstream of ARF7 and ARF19. These results indicate that the use of the LRIS provides a high reproducibility among divergent experiments, giving a high-resolution image on differential expression during lateral root initiation.

Cell Cycle Progression during Lateral Root Initiation

Within these 913 *LRI* genes, cell division–related genes were identified, such as *APC8/CDC23*, *PCNA1*, *RNR1*, *MCM3*, *MCM4*, *MCM7/PROLIFERA*, *RPS18A/PFL1*, *RPS13A/PFL2*, *FtsZ1-1*, *FtsZ2-1*, *CYCD3;2*, *CYCA2;4*, *CYCB2;5*, *CDKB2;1*, and *CKL3* (Table 1). APC8/CDC23 is part of the anaphase-promoting complex (APC) that is involved in targeting A- and B-type cyclins for degradation during mitosis (Capron et al., 2003). Proliferating cell nuclear antigen (PCNA1) belongs to the DNA replication machinery, and its expression is associated with the S phase (Hübscher et al., 2002). Minichromosome maintenance (MCM) proteins are conserved eukaryotic replication factors involved in the initiation of DNA replication (Stevens et al., 2002), and ribonucleotide reductase large subunit (RNR1) is part of a rate-limiting enzyme in the synthesis of nucleotides (Elledge et al., 1993). The ribosomal proteins encoded by *POINTED FIRST LEAVES1* (*PFL1*) and *PFL2* are produced during lateral root formation (Van Lijsebettens et al., 1994; Ito et al., 2000). FtsZ is involved in plastid divisions (Osteryoung et al., 1998). On the other hand, we recovered very few core cell cycle genes as defined by Vandepoele et al. (2002). The represented genes consisted of one G1-to-S (*CYCD3;2*), an S phase–related (*CYCA2;4*) and two G2-to-M–related genes (*CYCB2;5* and *CDKB2;1*), and a recently identified CDK-like protein-encoding gene (*CKL3*) (Menges et al., 2005). However, in the root part concerned, most core cell cycle genes are expressed in low abundance at this high stringency level ($P < 0.001$). When the stringency level was reduced to $P < 0.01$, the number of

Figure 3. (continued).

(A) Schematic representation of the cross-table clustering methodology. A two-series data set (wild type and *slr1*) of 3110 profiles is combined into a single-series data set corresponding to 6220 profiles irrespective of genotypic background. This data set was clustered into 14 clusters and includes the major patterns within the single-series data set. Subsequently, the clusters were plotted in a cross-table format: the wild-type and *slr1* expression clusters were plotted in front of the rows and at the head of the columns, respectively. All expression profiles over the different series are summarized by 14^2 (196) cluster combinations.

(B) Clusters illustrating the major patterns of the combined data set. In a white–gray gradient, the time points of the single series are shown. Each time point is characterized by the individual biological repeated values (0 h = 72 h NPA, 2 h = 0 h + 2 h NAA, and 6 h = 0 h + 6 h NAA). Clusters 1 to 6, 7 to 11, and 12 to 14 correspond to upregulated, constitutive, and downregulated expression profiles, respectively.

(C) Cross-table representation of the expression profiles within both genotypes. The frequencies of each cluster combination within the data set are indicated in each square. Gray marks no significant difference in induction rates between both genotypes, whereas red and orange and green and blue indicate that the induction rates are higher and lower in the wild type than in *slr1*, respectively. The black line outlines the selected 913 *LRI* genes.

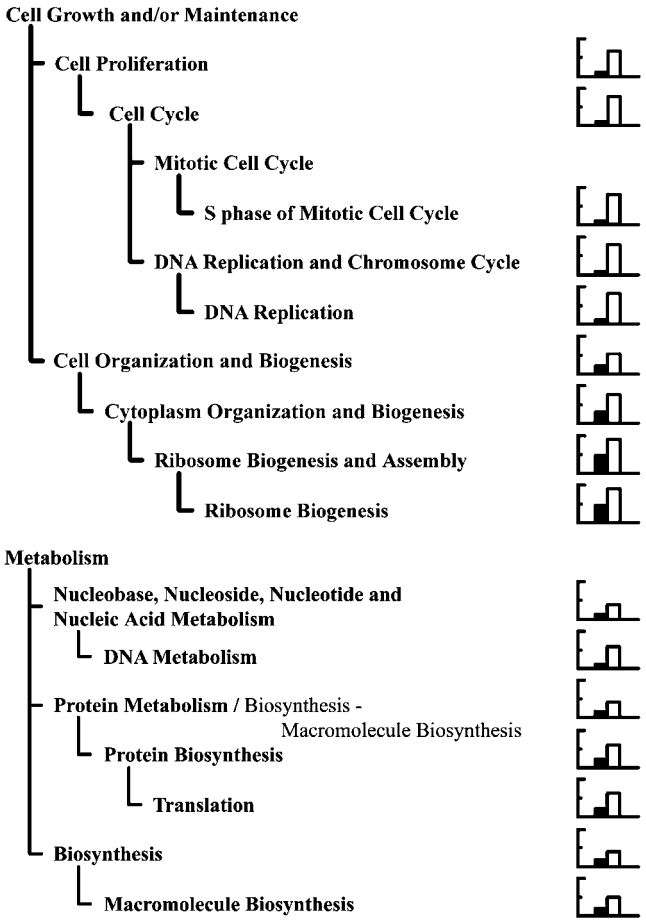

Figure 4. Overrepresented Functional Categories within the SLR/IAA14-Mediated Upregulated Genes.

For each significantly overrepresented functional category, the black and white bars represent the percentage of annotated genes within the 3110 significant genes versus all genes and within the 913 *LRI* genes versus the 3110 significant genes, respectively. Ordinate is 100%. The white bars illustrate the proportional enrichment of the genes in the functional categories when the selection is reduced from 3110 significant genes to 913 *LRI* genes.

significantly modulating cell cycle genes increased to 28 ($q < 0.05$) (see Supplemental Table 7 online).

Three cell cycle genes of the stringent selection, *CYCD3;2*, *CYCA2;4*, and *CDKB2;1*, contain at least one auxin-responsive element (ARE; TGTGTC or GAGACA) within a sequence 1000 bp upstream of their 5′ untranslated region (Figure 5A), suggesting that these genes may be part of the primary auxin response with their expression controlled by unstable AUX/IAA proteins (Ulmasov et al., 1997). Consistently, treating 5-d-old roots with the protein synthesis inhibitor cycloheximide (CHX) for 2 and 4 h resulted in a progressively strong induction of *CYCA2;4* and *CDKB2;1*, respectively (Figure 5B). However, for *CYCD3;2*, only a weak (nonsignificant) CHX-mediated induction was observed, suggesting that the AREs in its promoter may not be functional.

Consistent with the observation that their induction is strongly dependent on normal SLR/IAA14 degradation, *CYCA2;4* and *CDKB2;1* are probably directly regulated through a labile repressor, such as SLR/IAA14. Taken together, these results argue for a direct link between auxin signaling and cell cycle activation

Table 1. Known Auxin- and Cell Cycle–Related Genes within the *LRI* Genes

Description	Gene[a]	Arabidopsis Genome Initiative Code	Cluster Coordinates[b]
Cell cycle	*APC8/CDC23*	At3g48150	6.8
	PCNA1	At1g07370	3.6
	RNR1	At2g21790	3.8
	MCM3	At5g46280	3.8
	MCM4	At2g16440	3.6
	MCM7/PRL	At4g02060	3.8
	RPS18A/PFL1	At1g34030	6.8
	RPS13A/PFL2	At3g60770	6.8
	FtsZ1-1	At5g55280	6.9
	FtsZ2-1	At2g36250	6.8
	CYCD3;2	At5g67260	3.9
	CYCA2;4	At1g80370	2.9
	CKL3	At1g18670	2.4
	CYCB2;5	At1g20590	6.10
	CDKB2;1	At1g76540	6.10
Auxin signaling	***IAA1/AXR5***	At4g14560	2.4
	IAA4/AUX2-11	At5g43700	2.5
	IAA5/AUX2-27	At1g15580	3.6
	IAA11	At4g28640	1.2
	IAA13	At2g33310	2.4
	IAA18	At1g51950	4.8
	IAA19/MSG2	At3g15540	1.1
	IAA20	At2g46990	3.6
	IAA29	At4g32280	1.2
	ARF4	At5g60450	2.8
	ARF16	At4g30080	6.8
	ARF19	At1g19220	3.4
Auxin transport	*AUX1*	At2g38120	2.4
	LAX3	At1g77690	3.5
	PIN1	At1g73590	2.4
	PIN3	At1g70940	2.4
	PIN7	At1g23080	2.4
	PINOID/PID	At2g34650	1.1
	PINOID-like	At3g20830	4.8
	TCH3	At2g41100	2.4
	PGP1	At2g36910	4.8
Auxin conjugation	***GH3.1***	At2g14960	1.2
	GH3.3	At2g23170	1.1
	GH3.4	At1g59500	1.1
	GH3.5/AtGH3a	At4g27260	1.2
	GH3.6/DFL1	At5g54510	1.4
	UGT84B1	At2g23350	6.8
	IAR1	At1g51760	9.8
Auxin biosynthesis	CYP79B2	At4g39950	13.11
	CYP79B3	At2g22330	13.11
	ATR1	At5g60890	13.10
	YUCCA	At4g04180	4.2

[a] Genes in bold depend on ARF7 and ARF19 function for auxin inducibility (see Supplemental Table 6 online for expression profiles).
[b] Correspond to the clusters representing the expression profiles of the respective genes in Col-0 and in *slr1* (see Figure 3).

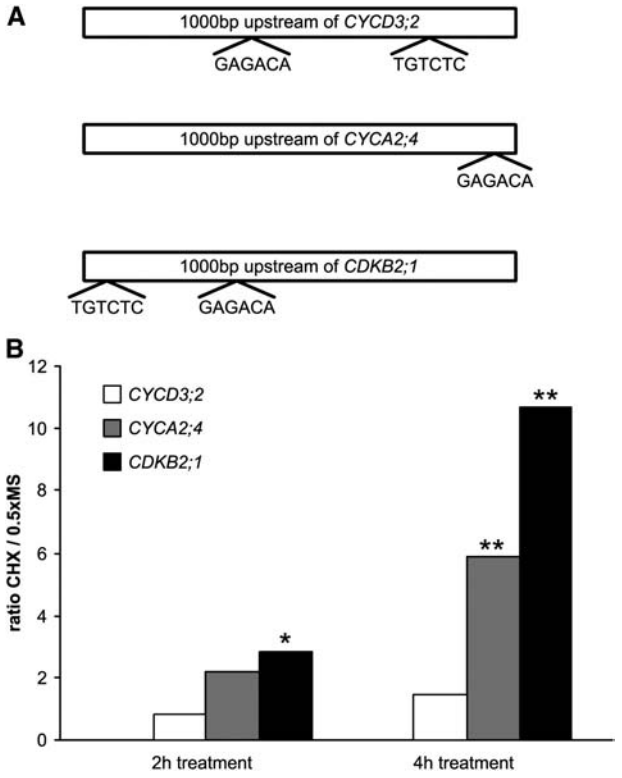

Figure 5. Analysis of Primary Auxin Responsiveness of *CYCD3;2*, *CYCA2;4*, and *CDKB2;1*.

(A) AREs within the 1000-bp sequence upstream of the 5′ untranslated region of *CYCD3;2*, *CYCA2;4*, and *CDKB2;1*.

(B) Ratios of mean expression levels for *CYCD3;2*, *CYCA2;4*, and *CDKB2;1* between CHX treatment and corresponding 0.5× Murashige and Skoog mock treatment for 2 and 4 h. The single asterisk and double asterisks indicate a significant difference between CHX-treated and mock-treated samples at $P < 0.05$ and $P < 0.005$, respectively.

during lateral root initiation both at the S phase and at the G2-to-M transition.

Cell Cycle Progression in the Pericycle Is Not Sufficient to Complement the Lack of Lateral Roots in *slr1*

Overexpression of G1/S regulators, such as *CYCD3;1* (Dewitte et al., 2003) or the transcription factor complex *E2Fa/DPa* (De Veylder et al., 2002), is sufficient to trigger several rounds of cell division in cell types that normally remain quiescent. Can overexpression of these cell cycle regulators induce pericycle cell proliferation and possibly even lateral roots in the absence of a normal SLR/IAA14-dependent auxin response? To address this question, *slr1* was crossed into the transgenic lines and their respective wild types. The root phenotypes of the F1 seedlings were analyzed in detail. All the wild-type (Columbia [Col-0] and Landsberg *erecta* [L*er*]) and *CYCD3;1*^{OE} (in L*er* background) plants formed normal roots (Figures 6A, 6E, and 6F). However, *E2Fa/DPa*^{OE} (in Col-0 background) showed a clear reduction in primary root length and in visible lateral roots (Figure 6B). The reduced lateral root density of *E2Fa/DPa*^{OE} was also observed in cleared 10-d-old roots and can be rescued by auxin treatment (I. De Smet, unpublished results). When *slr1* was crossed into Col-0, *E2Fa/DPa*^{OE}, L*er*, or *CYCD3;1*^{OE}, no lateral roots could be observed (Figures 6C, 6D, 6G, and 6H). Surprisingly, after closer microscopic inspection of the root, only in *CYCD3;1*^{OE} × *slr1* were regions seen in which the pericycle cells were shorter (Figure 6L) than those of mature L*er* and L*er* × *slr1* (Figures 6I and 6K). These series of short cells were found exclusively in the pericycle cell layer and are most probably the result of one or more extra rounds of cell division. In *E2Fa/DPa*^{OE} × *slr1* and Col-0 × *slr1* roots, no such regions with shortened pericycle cells could be observed (data not shown). Unlike in a stage I primordium, which is normally composed of small radially swollen cells in the midst of larger elongated cells (Figure 6J; Malamy and Benfey, 1997), the short pericycle cells in *CYCD3;1*^{OE} × *slr1* roots had a uniform cell size and were not radially swollen (Figure 6L). Also absent were stage II lateral root primordia, which are the result of a periclinal division of stage I primordium cells. To verify whether these regions of shortened cells were the consequence of extra rounds of cell division after leaving the meristem, the expression levels of the S phase–associated *CYCA2;4* gene (Figure 6M) and G2/M-specific *CYCB1;1* (Figure 6N) and *CYCB2;5* (Figure 6O) were analyzed via real-time RT-PCR in the *CYCD3;1*^{OE} × *slr1* background. In *slr1* background, the expression of these cell cycle genes was strongly reduced, whereas that of both genes appeared to be restored by *CYCD3;1* overexpression. To assess whether this cell division activity in the pericycle of the mutant was associated with a recovered capacity to initiate a new organ, the expression of the *PLETHORA1* (*PLT1*) gene was analyzed in *CYCD3;1*^{OE} × *slr1* roots. *PLT1* encodes a transcription factor that has been shown to be associated with quiescent center specification downstream of the auxin signal (Aida et al., 2004). Because a new quiescent center has to be specified during lateral root formation, *PLT1* expression can be used as a marker for early stages of lateral root organogenesis (see Supplemental Figure 2 online). Nevertheless, *PLT1* expression remained low in *CYCD3;1*^{OE} × *slr1* roots (Figure 6P). These results indicate that the requirements for organogenetic processes, such as lateral root initiation, are more complex than simple activation of the cell cycle and that additional SLR/IAA14-dependent signaling is needed to develop a new organ.

Complex Auxin Signaling-Dependent Mechanisms Regulate Lateral Root Initiation

As expected, besides cell cycle–related genes, several central regulators of auxin signaling were recovered among the *LRI* genes (Table 1). Nine *AUX/IAA* genes were identified within this selection. For two of them, gain-of-function mutants with defects in lateral root formation have been described before (*axr5/iaa1* [Park et al., 2002; Yang et al., 2004] and *msg2-1/iaa19* [Tatematsu et al., 2004]). The remaining seven *AUX/IAA* genes have not been characterized functionally. In addition to this type of negative feedback regulation, several potential *AUX/IAA* targets, such as *ARF4*, *ARF16*, and *ARF19*, were also strongly upregulated in a SLR/IAA14-dependent fashion, especially

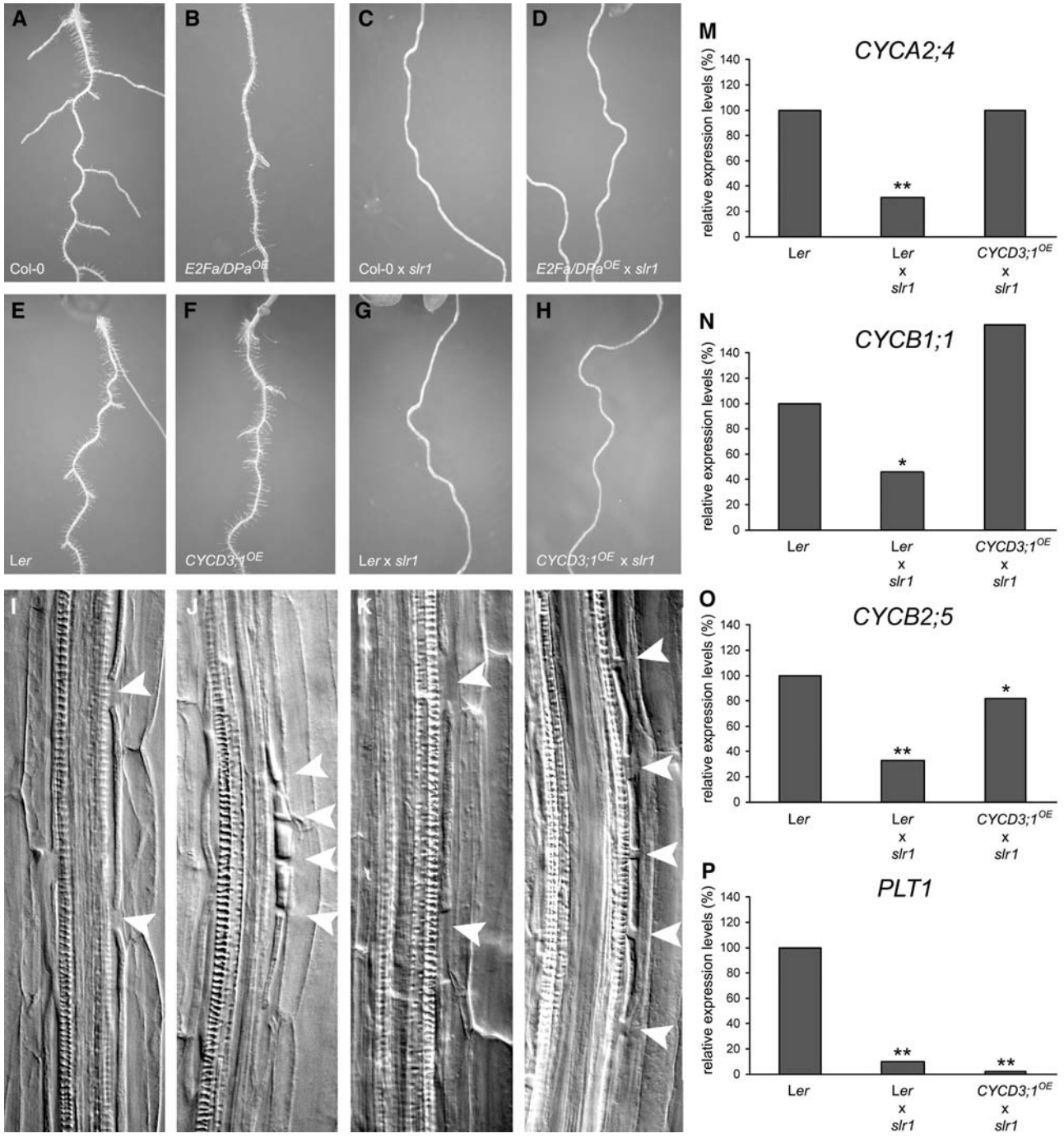

Figure 6. Complementation of Cell Cycle Defect in *slr1*.

(A) to **(H)** Overview of root phenotypes of 5-d-old seedlings of Col-0 **(A)**, *E2Fa/DPa*^{OE} **(B)**, Col-0 × *slr1* **(C)**, *E2Fa/DPa*^{OE} × *slr1* **(D)**, L*er* **(E)**, *CYCD3;1*^{OE} **(F)**, L*er* × *slr1* **(G)**, and *CYCD3;1*^{OE} × *slr1* **(H)**.

(I) to **(L)** Microscopic analysis of the pericycle after clearing of mature L*er* pericycle cell **(I)**, L*er* stage I lateral root primordium **(J)**, mature L*er* × *slr1* pericycle cell **(K)**, and zone of shortened pericycle cells in *CYCD3;1*^{OE} × *slr1* **(L)**. Arrowheads mark pericycle cell size.

(M) to **(P)** Real-time PCR analysis on L*er*, L*er* × *slr1*, and *CYCD3;1*^{OE} × *slr1* roots of *CYCA2;4* **(M)**, *CYCB1;1* **(N)**, *CYCB2;5* **(O)**, and *PLT1* **(P)**. The single asterisk and double asterisks indicate significant reduction of expression compared with L*er* at $P < 0.01$ and $P < 0.001$, respectively.

ARF19, which seems to play an important role in regulating lateral root formation because *arf7 arf19* double mutants exhibit an *slr1*-like phenotype (Okushima et al., 2005; Wilmoth et al., 2005). Furthermore, both ARF7 and ARF19 were shown to interact with SLR/IAA14 in a yeast two-hybrid assay (Fukaki et al., 2005). In conclusion, our microarray data show SOLITARY ROOT/IAA14-dependent expression of both *AUX/IAA* and *ARF* genes, suggesting that at the level of auxin signaling, lateral root initiation is tightly regulated through both negative and positive feedback.

Attenuating and Maintaining Auxin Levels during Lateral Root Initiation

Auxin conjugation, transport, and biosynthesis contribute to local auxin homeostasis. The data set presented (Table 1) indicates that these three processes are a part of lateral root initiation.

The *GH3* gene family consists of the first identified auxin-responsive genes (Hagen et al., 1991) and has been divided into three major groups, according to their substrate specificity and sequence similarities (Staswick et al., 2002). Six group II GH3 proteins have been shown to act as IAA-amido synthetases, providing a mechanism to reduce the level of active auxin by conjugation to amino acids (Staswick et al., 2005). Interestingly, all five *GH3* genes identified as *LRI* genes belong to the group II GH3 family, and besides ARF8 (Tian et al., 2004), they also seem to be regulated through ARF7 and ARF19 transcription factors (Okushima et al., 2005). Also, *UGT84B1*, coding for an enzyme involved in the conjugation of glucose to IAA (Jackson et al., 2002), was induced in the wild type, but not in *slr1*. By contrast, *IAR1*, which codes for a putative ZIP family transporter protein and is necessary for the production of IAA out of IAA–amino acid conjugates (Lasswell et al., 2000), was strongly repressed in the wild type and to a lesser extent in *slr1*. A negative feedback mechanism interfering with the level of free auxin is therefore likely to be active during lateral root initiation.

On the other hand, many components of the auxin transport machinery were recovered within the *LRI* genes. Not only did the putative auxin influx carriers *AUX1* and *Like-AUX1 3* (*LAX3*) (Parry et al., 2001) emerge, but so did the auxin efflux facilitators, such as *PIN1*, *PIN3*, and *PIN7* (Paponov et al., 2005), and some proteins involved in their correct localization, such as PINOID/PID (Friml et al., 2004), PINOID-like, and a PID-interacting protein, TCH3 (Benjamins et al., 2003). Moreover, the multidrug resistance protein involved in polar auxin transport encoded by *PGP1* (Lin and Wang, 2005) was found among the *LRI* genes. The corresponding mutants display defects in lateral root initiation (Bennett et al., 1996; Benková et al., 2003). The auxin inducibility of polar auxin transport genes (influx and efflux) was also observed within the vascular cambium of hybrid aspen (Schrader et al., 2003). Interestingly, *PIN1*, *PIN3*, and *PIN7* were also shown to depend on ARF7 and ARF19 for their auxin inducibility (Okushima et al., 2005), and their AUX/IAA-dependent inducibility has been implicated in their functional redundancy (Vieten et al., 2005).

Recently, auxin has been shown to negatively regulate its own biosynthesis (Ljung et al., 2005). Two genes encoding enzymes involved in the Trp-dependent IAA biosynthesis pathway (*CYP79B2* and *CYP79B3*) (Zhao et al., 2002) and their transcriptional regulator *ATR1/MYB34* (Celenza et al., 2005) were downregulated upon auxin treatment in the wild type, but to a lesser extent in *slr1*. Interestingly, *YUCCA*, a gene encoding another rate-limiting enzyme of the Trp-dependent IAA biosynthesis pathway (Zhao et al., 2001), was more induced in *slr1* than in the wild type.

Taken together, these data suggest that auxin homeostasis is disturbed in *slr1*. Therefore, the auxin content of seedling roots of the wild type and *slr1* was determined by gas chromatography–selected reaction monitoring–mass spectrometry (Ljung et al., 2005). Indeed, a significantly higher auxin concentration was found in the most apical 3 mm of *slr1* primary roots than those of the wild type ($P < 0.005$; Figure 7A). Correspondingly, the increased auxin concentration in *slr1* could be visualized with P_{DR5}:*GUS* (Figures 7B to 7E).

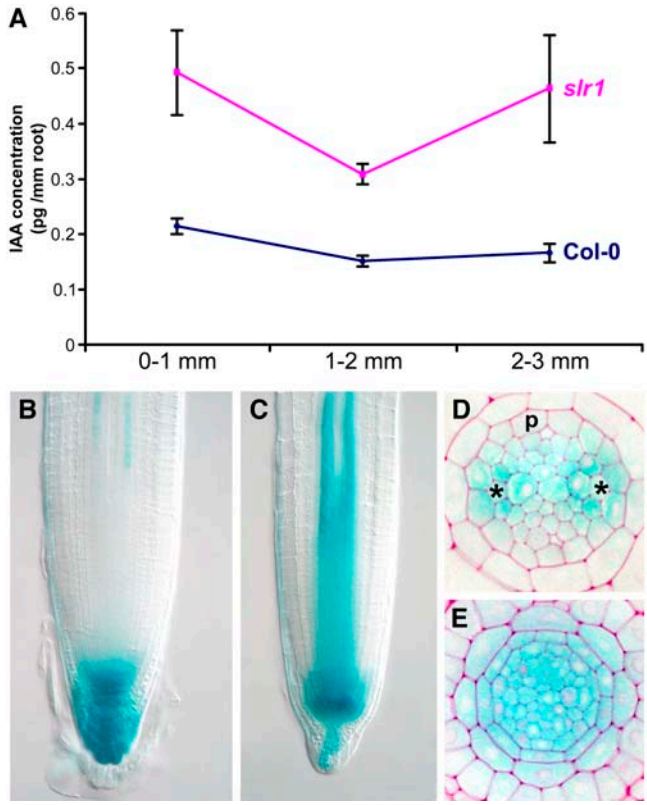

Figure 7. Analysis of Auxin Content in Col-0 and *slr1*.

(A) IAA concentration of Col-0 and *slr1* of the 3-mm most apical part of the primary root. Standard deviations are indicated by error bars.

(B) and **(C)** P_{DR5}:*GUS* expression in 5-d-old root apical meristems in Col-0 and *slr1*, respectively.

(D) and **(E)** Anatomical analysis of P_{DR5}:*GUS* in *slr1* of the elongation zone and the root apical meristem, respectively. p, pericycle. The asterisks indicate protoxylem cells.

DISCUSSION

The results of our genome-wide transcriptome analysis allow us to present a model describing a regulatory network that integrates some of the most likely occurring processes upon auxin perception during the onset of lateral root initiation (Figure 8). The auxin signaling cascade starts off by the auxin-stimulated targeting of AUX/IAA proteins for degradation, thereby derepressing the transcriptional activity of ARFs (reviewed in Dharmasiri and Estelle, 2004). Therefore, the auxin-mediated degradation of the SLR/IAA14 protein might be the first crucial event in the preamble toward lateral root initiation (Figure 8A).

The Importance of Cell Cycle Progression during Lateral Root Initiation

When the auxin-induced transcriptional changes in root segments of the wild type and *slr1* are compared, the inhibition of auxin signal transduction in the mutant is correlated with the failure to induce cell cycle–related genes. Although the role of auxin in cell cycle progression is generally accepted, we found evidence that this stimulation may occur via an AUX/IAA-ARF–dependent pathway. Indeed, *CYCA2;4* and *CDKB2;1* both contain at least one ARE in their promoter sequence, and their auxin inducibility has been shown to depend on the normal degradation of SLR/IAA14. Furthermore, both genes are induced by the inhibition of protein synthesis, suggesting that a labile repressor is controlling their transcription. Because AUX/IAA proteins are regarded as labile repressors (Ouellet et al., 2001), it is tempting to consider *CYCA2;4* and *CDKB2;1* to be primary targets of the SLR/IAA14 signaling. These results are indicative for a potential molecular mechanism by which auxin signaling may feed into the cell cycle. Nevertheless, the functionality of the respective AREs remains to be proven.

However, stimulation of the cell cycle was not sufficient to trigger the formation of lateral roots in the *slr1* background.

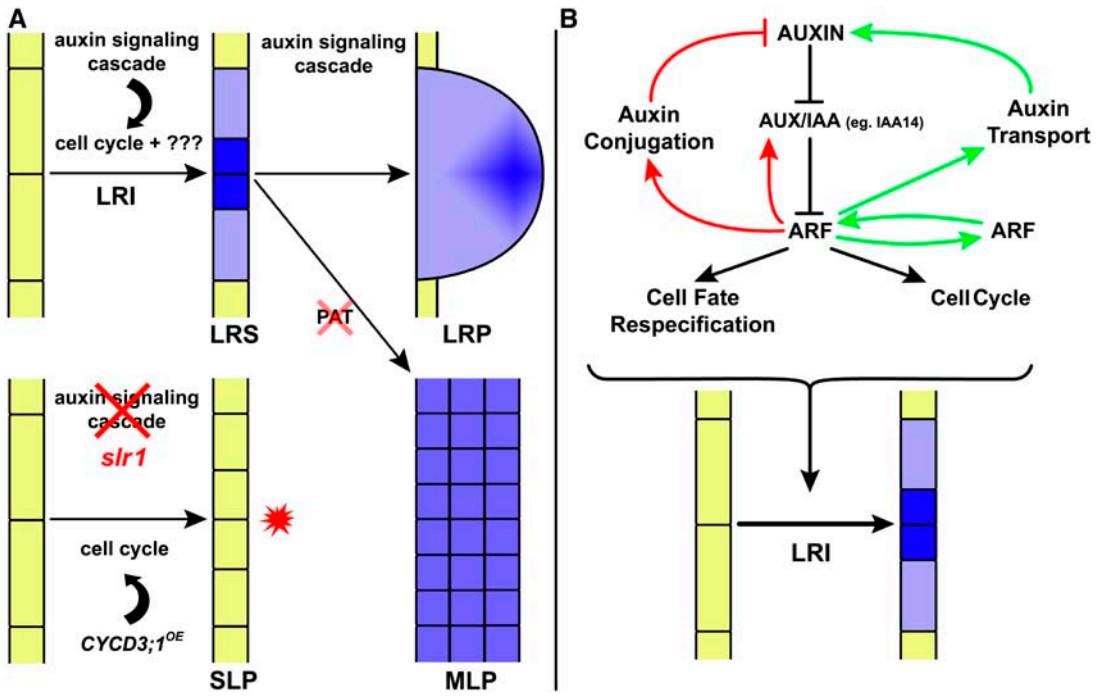

Figure 8. Model of SLR/IAA14-Dependent Lateral Root Initiation.

(A) Induction of lateral root initiation (LRI) in the pericycle, resulting in a lateral root initiation site (LRS) when the auxin signaling cascade is intact. Further development toward a lateral root primordium is also dependent on auxin. When the polar auxin transport machinery is intact, auxin gradients are set up to organize the lateral root primordium (LRP). Disturbing the polar auxin transport (PAT) does not inhibit the auxin-induced developmental program of lateral root formation but provokes, rather, an unorganized multilayered proliferating zone (MLP) (Benková et al., 2003; Geldner et al., 2004). When the auxin signaling cascade is defective (*slr1*), no lateral roots can be initiated. Complementation of the cell cycle defect in *slr1* by overexpression of *CYCD3;1* is not sufficient to activate the developmental program of LRI; nevertheless, it can induce some proliferative divisions in the pericycle, resulting in a single-layered proliferating zone (SLP).

(B) Model for AUX/IAA-mediated lateral root initiation (LRI). Black path: in the early auxin signaling cascade, increased auxin levels stimulate the degradation of AUX/IAA proteins, such as SLR/IAA14. AUX/IAA proteins repress the transcriptional activity of one or more ARFs. Downstream of this signaling cascade lies the activation of the developmental program of lateral root initiation that includes the coordinated action of cell fate respecification and cell cycle progression. Red paths: the auxin signaling cascade induces auxin conjugation and may negatively influence auxin content. Also, increased auxin levels induce AUX/IAA proteins that repress ARF transcriptional activity. Green paths: increased auxin levels can induce auxin transport, leading to even higher auxin levels. Furthermore, auxin induces ARF production, promoting downstream auxin signal transduction.

Only *CYCD3;1*^{OE} was capable of initiating a round of cell divisions in *slr1* pericycle cells, giving rise to a single layered proliferation zone (Figure 8A) that did not progress further into lateral root developmental stages, let alone lateral root primordia.

Cell Fate Respecification of the Pericycle

The inability to form lateral roots after cell cycle stimulation of the pericycle suggests that besides cell cycle progression, *slr1* is unable to respecify the identity of pericycle cells into that of lateral root primordia. Analogous to the situation found in early embryogenesis, the formation of lateral roots also seems to depend on cell fate alteration through the occurrence of asymmetric divisions. In case of embryogenesis and primary root development, polar auxin transport installs an auxin maximum, visualized by the auxin reporter construct P_{DR5}:*GUS* (Sabatini et al., 1999), restricting *PLT* expression that specifies stem cell identity (Aida et al., 2004; Blilou et al., 2005). Likewise, polar auxin transport is required to form lateral roots because mutants defective in polar auxin transport fail to produce lateral roots (Benková et al., 2003; Geldner et al., 2004). Transcripts of the polar auxin transport machinery appear to be unable to accumulate normally in auxin-treated *slr1* roots, preventing the installation of an auxin maximum. Therefore, it might be argued that fine-tuned polar auxin transport could be the missing factor to specify stem cell identity for lateral root initiation in *slr1*. Other mutants defective in polar auxin transport were unable to produce individual lateral root primordia upon auxin supplementation; instead, multilayered proliferation zones (Figure 8A) developed (Benková et al., 2003; Geldner et al., 2004). Nevertheless, none were detected in the *slr1* root that has increased auxin levels, even when cell division was stimulated by *CYCD3;1*^{OE}. However, *PLT* expression was not restored by *CYCD3;1*^{OE} in *slr1*, suggesting that the induced pericycle cell divisions do not correspond to lateral initiation sites. Thus, the impaired auxin transport in *slr1* would probably not be the only element responsible for its inability to form lateral roots. Polar auxin transport is necessary for providing auxin to the pericycle and for organizing the auxin gradient in the developing lateral root primordium; induction of other factors are probably also needed to turn into organogenesis.

Such factors, which are indispensable for induction of asymmetric divisions, acquisition of different cell fates, and organogenesis, might be represented by members of the *WUSCHEL-related homeobox* (*WOX*) family. During embryogenesis, *WOX* genes are expressed in restricted areas of the embryo and are believed to be involved in cell fate specification (Haecker et al., 2004). In this respect, it is worth mentioning that one member of the *WOX* family, *WOX13*, was retrieved among the *LRI* genes. The SLR/IAA14-mediated auxin inducibility (cluster combination 6.8) of *WOX13* suggests that it is involved in the respecification of pericycle cells during lateral root initiation. Moreover, the functional analysis of other proteins encoded by the *LRI* genes will probably result in the identification of potential cell fate respecification factors and will provide new insights into this intriguing developmental process.

A Binary Switch Mechanism Is Involved in Lateral Root Initiation

Our results suggest that lateral root initiation is regulated through positive as well as negative feedback loops (Figure 8B, green and red arrows). Two types of regulation with negative effects on auxin concentration and/or signal transduction can be distinguished from the data set (Figure 8B, red arrows). One type is brought about by the strong upregulation of genes encoding enzymes involved in auxin conjugation. Conjugation of IAA to amino acids or sugars can reduce the free auxin level, although some conjugates of IAA and amino acids are reversible and can contribute to the pool of free IAA (Rampey et al., 2004). However, the contribution of IAA oxidation is believed to be much more important for auxin homeostasis than that of conjugation (Kowalczyk and Sandberg, 2001). Secondly, in contrast with the auxin-induced instability of AUX/IAA proteins (Gray et al., 2001), their expression was found to be strongly induced within the LRIS. Because these proteins encode potent inhibitors of ARF-mediated transcription (Tiwari et al., 2004), their induction provides a direct negative feedback onto the auxin signal transduction.

An example of a positive feedback loop (Figure 8B, green arrows) is the active auxin transport that has been shown to be auxin inducible in a SLR/IAA14-dependent manner. The installation of its own transport machinery matches the self-organizing nature of auxin transport suggested in the canalization hypothesis proposed by Sachs (1988). This supposition implies that high auxin levels in the pericycle would be actively reinforced by the locally increased auxin transport potential. Furthermore, the downregulation of IAA biosynthesis genes and the upregulation of the IAA conjugation potential in early stages of lateral root initiation suggest that young primordia depend on auxin import for their development. Later on, in emerged lateral root primordia, a regained capacity for auxin biosynthesis has been observed (Ljung et al., 2005). Indeed, only excised lateral root primordia at later stages of development can grow in culture without added hormones (Laskowski et al., 1995). Furthermore, expression of several ARFs is also induced during lateral root initiation, reducing the AUX/IAA versus ARF ratio with an increased sensitivity toward auxin as a consequence and amplification of the auxin signal to stimulate the onset of lateral root initiation.

In summary, in the proposed model, lateral root initiation is subjected to two counteracting regulatory circuits that result in a binary switch mechanism. When the auxin concentration is low, the auxin response acts to dampen small fluctuations in auxin concentration and no lateral roots are initiated. When this negative regulation is overcome, auxin concentration and responsiveness are actively reinforced by a positive feedback mechanism. This positive spiral activates the developmental program of lateral root initiation. When *SLR/IAA14* is mutated, no lateral roots can be produced. Also, auxin homeostasis is misregulated in *slr1*, leading to auxin accumulation. Thus, our model is consistent with the experimental data and provides a basis to understand the complex self-regulatory mechanisms involved in lateral root initiation.

METHODS

Plant Material and Growth Conditions

In this study, we analyzed the *Arabidopsis thaliana* Heynh. ecotypes Col-0 and L*er*, the mutant *slr1* (Fukaki et al., 2002), the promoter fusions P_{IAA14}:*GUS* (Fukaki et al., 2002), $P_{CDKA;1(cdc2a)}$:*GUS* (Hemerly et al., 1993), $P_{CDKB1;1}$:*GUS* (de Almeida Engler et al., 1999), $P_{CYCB1;1}$:*GUS* (Colón-Carmona et al., 1999), P_{DR5}:*GUS* (Ulmasov et al., 1997), P_{ALF4}:*GUS* (DiDonato et al., 2004), *E2Fa/DPa*^{OE} (De Veylder et al., 2002), *CYCD3;1*^{OE} (Dewitte et al., 2003), and the xylem pole pericycle-specific GAL4 enhancer trap line J0121 (http://www.plantsci.cam.ac.uk/Haseloff/geneControl/catalogues/Jlines/record/record_0.html). Seeds were always germinated on medium derived from standard Murashige and Skoog medium on vertically oriented square plates (Greiner Labortechnik) in a growth chamber under continuous light (110 $\mu E \cdot m^{-2} \cdot s^{-1}$ photosynthetically active radiation, supplied by cool-white fluorescent tungsten tubes; Osram) at 22°C (Himanen et al., 2002). Supplements consisted of 10 μM NPA (Duchefa), 10 μM NAA (Sigma-Aldrich), or 30 μM CHX (Sigma-Aldrich).

Histochemical and Histological Analysis

The GUS assays were performed as described by Beeckman and Engler (1994). For microscopic analysis, samples were cleared by mounting in 90% lactic acid (Acros Organics) (analysis of GUS stainings) or using the clearing method described by Malamy and Benfey (1997) (analysis of pericycle cell length). All samples were analyzed by differential interference contrast microscopy (Leica DMLB).

For anatomical sections, GUS-stained samples were fixed overnight in 1% glutaraldehyde and 4% paraformaldehyde in 50 mM phosphate buffer, pH 7. Samples were dehydrated and embedded in Technovit 7100 resin (Heraeus Kulzer) according to the manufacturer's protocol. For proper orientation of the samples, we used a two-step embedding methodology, based on a pre-embedding step to facilitate orientation in 0.5-mL Eppendorf tubes (De Smet et al., 2004). Sections of 5 μm were cut with a microtome (Minot 1212; Leitz), dried on Vectabond-coated object glasses, counterstained for cell walls with 0.05% ruthenium red for 8 min (Fluka Chemica), and rinsed in tap water for 30 s. After drying, the sections were mounted in DePex medium (British Drug House) and covered with cover slips.

Photographs were taken with a CAMEDIA C-3040 zoom digital camera (Olympus) and processed with Photoshop 7.0 (Adobe Systems).

Microarray Analysis and Data Processing

Col-0 and *slr1* seeds were germinated on medium containing 10 μM NPA and transferred 3 d after germination under continuous light to 10 μM NAA, according to the points of the time course (0, 2, and 6 h). All sampling points were performed in duplicate. For each sampling, ~1000 root segments between root apical meristem and root-hypocotyl junction were pooled. From the pooled LRIS, RNA of root segments was extracted with the RNeasy kit (Qiagen). Out of 5.8 μg of total RNA, biotinylated copy RNA was produced (Hennig et al., 2003), of which 20 μg was fragmented and hybridized to the ATH1 arrays (Affymetrix). Washing, detection, and scanning were performed as described by Hennig et al. (2003). Raw data were processed with the statistical algorithm of the Affymetrix Microarray Suite 5.0 (Liu et al., 2002). Box plots of $\log_2$-transformed normalized value distributions of all arrays show that most array-to-array effects were taken care of by the normalization procedure (see Supplemental Figure 3 online). The normalized data were subjected to two-factor analysis of variance with Microsoft Excel. The false positives were controlled by measuring the false discovery rate (q-value) (Storey and Tibshirani, 2003) with the freely available software QVALUE (http://genomine.org/qvalue/). Significant profiles were preprocessed (Figure 3A) prior to clustering. The optimal number of clusters was estimated with the figure of merit calculations (Yeung et al., 2001) and K means clustered (Soukas et al., 2000) in the Multiple Experiment Viewer 2.2 of The Institute for Genome Research (Saeed et al., 2003). The cross-table was constructed with Photoshop 7.0.

Real-Time PCR

RNA was extracted with the RNeasy kit. Poly(dT) cDNA was prepared from 1 μg of total RNA with Superscript III reverse transcriptase (Invitrogen) and quantified on an iCycler apparatus (Bio-Rad) with the qPCR core kit for SYBR green I (Eurogentec). PCR was performed in 96-well optical reaction plates heated for 10 min to 95°C to activate hot start Taq DNA polymerase, followed by 50 cycles of denaturation for 60 s at 95°C and annealing extension for 60 s at 58°C. Target quantifications were performed with specific primer pairs designed with the Beacon Designer 4.0 (Premier Biosoft International). All PCRs were performed in triplicate. Expression levels were first normalized to *ACTIN2* expression levels that did not show clear systematic changes in Ct value and then to the respective expression levels in the wild type (L*er*). The primers used to quantify gene expression levels were At1g42970/*GAPDH*, 5′-TCTTTCCCTGCTCAATGCTCCTC-3′ and 5′-TTTCGCCACTGTCTCTCCTCTAAC-3′; At3g18780/*ACTIN2*, 5′-TTGACTACGAGCAGGAGATGG-3′ and 5′-ACAAACGAGGGCTGGAACAAG-3′; At1g80370/*CYCA2;4*, 5′-GCTCCAGATCGCCTCCAAG-3′ and 5′-CACGCAGGTTGTAGTAGATG-3′; At1g20590/*CYCB2;5*, 5′-GAGTTTCACACAGGCTAC-3′ and 5′-AGATGTGTTGTACTTCCTG-3′; and At3g20840/*PLT1*, 5′-ACGATATGCCTTCCAGTGATG-3′ and 5′-TTCAGACCCATTCCTTGTGC-3′.

Quantification of IAA

Wild-type and mutant *slr1* seedlings were grown on vertical plates (1× Murashige and Skoog medium, 1% sucrose, and 1% agar, pH 5.7) under long-day conditions (16 h light, 8 h darkness). Samples were collected, extracted, and purified as described by Ljung et al. (2005). Of the primary root, the apical 3 mm was collected from 7-d-old seedlings and cut in 1-mm sections. For each sample, sections from 50 seedlings were pooled. Endogenous IAA content was analyzed by gas chromatography–selected reaction monitoring–mass spectrometry (Edlund et al., 1995). Isotopic dilution was calculated based on the addition of 100 pg $^{13}C_6$-IAA per sample. Four replicates were analyzed for each sample.

Accession Numbers and Data Deposition

All microarray data will be available in the Genevestigator database (Zimmermann et al., 2004; https://www.genevestigator.ethz.ch) and in the public repository Gene Expression Omnibus upon publication (http://www.ncbi.nlm.nih.gov/geo/) under accession number GSE3350. The accession numbers of the genes used in this study are At4g14550 (*SLR/IAA14*), At3g54180 (*CDKB1;1*), At3g48750 (*CDKA;1*), At4g37490 (*CYCB1;1*), At4g34160 (*CYCD3;1*), At2g36010 (*E2Fa*), At5g02470 (*DPa*), At5g20730 (*ARF7*), At5g37020 (*ARF8*), At5G11030 (*ALF4*), At3G20840 (*PLT1*), and At4g35550 (*WOX13*). Accession numbers of other genes discussed in the text are listed in Table 1.

Supplemental Data

The following materials are available in the online version of this article.

Supplemental Table 1. List of the 3110 Significant Genes.

Supplemental Table 2. List of the 913 Lateral Root Initiation Genes.

Supplemental Table 3. Overrepresented Gene Ontology Functional Categories of *LRI* Genes versus All Significant Genes and of the Early Induced *LRI* Genes versus All Significant Genes.

Supplemental Table 4. Overlapping Upregulated Genes between This Study and That of Himanen et al. (2004) with the Cluster Combination and the Cluster Number and Profile, Respectively.

Supplemental Table 5. Expression Profiles of the *LRI* Genes in the *arf7 arf19* Data Set from Okushima et al. (2005).

Supplemental Table 6. *LRI* Genes with *arf7 arf19*–Dependent Auxin Inducibility.

Supplemental Table 7. Cell Cycle Genes Differentially Regulated at a Stringency Level of $P < 0.01$.

Supplemental Figure 1. P_{IAA14}*:GUS* Activity throughout Different Stages of Lateral Root Development.

Supplemental Figure 2. Histochemical Localization of *plt1-1*::*GUS* Activity Using a Promoter-Trap Line during Different Stages of Lateral Root Formation.

Supplemental Figure 3. Box Plots of Log_2-Transformed Normalized Value Distributions of All Arrays.

ACKNOWLEDGMENTS

We thank Satoshi Tameda for GUS staining, Gun Löfdahl and Marzanna Gontarczyk for skillful technical assistance, the Nottingham Arabidopsis Stock Centre, the ABRC, Peter Doerner, John Celenza, Tom Guilfoyle, and Jim Murray for sharing material, Ben Scheres and Jiří Friml for critical reading of the manuscript, and Martine De Cock for help in preparing it. This work was supported by a grant from the Interuniversity Poles of Attraction Program–Belgian Science Policy (P5/13), in part by Grant-in-Aid for Scientific Research on Priority Areas (Molecular Basis of Axis and Signals in Plant Development) and for Scientific Research for Young Scientists from the Ministry of Education, Culture, Sports, Science, and Technology of Japan to H.F., and a grant from the Research for the Future program of the Japan Society for the Promotion of Science to M.T. S.V. and I.D.S. are indebted to the Institute for the Promotion of Innovation through Science and Technology in Flanders for predoctoral fellowships.

Received June 24, 2005; revised August 22, 2005; accepted September 26, 2005; published October 21, 2005.

REFERENCES

Aida, M., Beis, D., Heidstra, R., Willemsen, V., Blilou, I., Galinha, C., Nussaume, L., Noh, Y.-S., Amasino, R., and Scheres, B. (2004). The *PLETHORA* genes mediate patterning of the *Arabidopsis* root stem cell niche. Cell **119,** 109–120.

Beeckman, T., Burssens, S., and Inzé, D. (2001). The peri-cell-cycle in *Arabidopsis.* J. Exp. Bot. **52,** 403–411.

Beeckman, T., and Engler, G. (1994). An easy technique for the clearing of histochemically stained plant tissue. Plant Mol. Biol. Rep. **12,** 37–42.

Benjamins, R., Galván Ampudia, C.S., Hooykaas, P.J.J., and Offringa, R. (2003). PINOID-mediated signaling involves calcium-binding proteins. Plant Physiol. **132,** 1623–1630.

Benková, E., Michniewicz, M., Sauer, M., Teichmann, T., Seifertová, D., Jürgens, G., and Friml, J. (2003). Local, efflux-dependent auxin gradients as a common module for plant organ formation. Cell **115,** 591–602.

Bennett, M.J., Marchant, A., Green, H.G., May, S.T., Ward, S.P., Millner, P.A., Walker, A.R., Schulz, B., and Feldmann, K.A. (1996). *Arabidopsis AUX1* gene: A permease-like regulator of root gravitropism. Science **273,** 948–950.

Berardini, T.Z., et al. (2004). Functional annotation of the Arabidopsis genome using controlled vocabularies. Plant Physiol. **135,** 745–755.

Blilou, I., Xu, J., Wildwater, M., Willemsen, V., Paponov, I., Friml, J., Heidstra, R., Aida, M., Palme, K., and Scheres, B. (2005). The PIN auxin efflux facilitator network controls growth and patterning in *Arabidopsis* roots. Nature **433,** 39–44.

Capron, A., Serralbo, O., Fülöp, K., Frugier, F., Parmentier, Y., Dong, A., Lecureuil, A., Guerche, P., Kondorosi, E., Scheres, B., and Genschik, P. (2003). The Arabidopsis anaphase-promoting complex or cyclosome: Molecular and genetic characterization of the APC2 subunit. Plant Cell **15,** 2370–2382.

Casimiro, I., Beeckman, T., Graham, N., Bhalerao, R., Zhang, H., Casero, P., Sandberg, G., and Bennett, M.J. (2003). Dissecting *Arabidopsis* lateral root development. Trends Plant Sci. **8,** 165–171.

Casimiro, I., Marchant, A., Bhalerao, R.P., Beeckman, T., Dhooge, S., Swarup, R., Graham, N., Inzé, D., Sandberg, G., Casero, P.J., and Bennett, M. (2001). Auxin transport promotes Arabidopsis lateral root initiation. Plant Cell **13,** 843–852.

Celenza, J.L., Quiel, J.A., Smolen, G.A., Merrikh, H., Silvestro, A.R., Normanly, J., and Bender, J. (2005). The Arabidopsis ATR1 Myb transcription factor controls indolic glucosinolate homeostasis. **137,** 253–262.

Colón-Carmona, A., You, R., Haimovitch-Gal, T., and Doerner, P. (1999). Spatio-temporal analysis of mitotic activity with a labile cyclin-GUS fusion protein. Plant J. **20,** 503–508.

de Almeida Engler, J., De Vleesschauwer, V., Burssens, S., Celenza, J.L. Jr., Inzé, D., Van Montagu, M., Engler, G., and Gheysen, G. (1999). Molecular markers and cell cycle inhibitors show the importance of cell cycle progression in nematode-induced galls and syncytia. Plant Cell **11,** 793–807.

De Paepe, A., Vuylsteke, M., Van Hummelen, P., Zabeau, M., and Van Der Straeten, D. (2004). Transcriptional profiling by cDNA-AFLP and microarray analysis reveals novel insights into the early response to ethylene in *Arabidopsis.* Plant J. **39,** 537–559.

De Smet, I., Chaerle, P., Vanneste, S., De Rycke, R., Inzé, D., and Beeckman, T. (2004). An easy and versatile embedding method for transverse sections. J. Microsc. **213,** 76–80.

De Veylder, L., Beeckman, T., Beemster, G.T.S., de Almeida Engler, J., Ormenese, S., Maes, S., Naudts, M., Van Der Schueren, E., Jacqmard, A., Engler, G., and Inzé, D. (2002). Control of proliferation, endoreduplication and differentiation by the *Arabidopsis* E2Fa/DPa transcription factor. EMBO J. **21,** 1360–1368.

De Veylder, L., Beeckman, T., Beemster, G.T.S., Krols, L., Terras, F., Landrieu, I., Van Der Schueren, E., Maes, S., Naudts, M., and Inzé, D. (2001). Functional analysis of cyclin-dependent kinase inhibitors of Arabidopsis. Plant Cell **13,** 1653–1667.

De Veylder, L., Segers, G., Glab, N., Casteels, P., Van Montagu, M., and Inzé, D. (1997). The *Arabidopsis* Cks1At protein binds to the cyclin-dependent kinases Cdc2aAt and Cdc2bAt. FEBS Lett. **412,** 446–452.

Dewitte, W., Riou-Khamlichi, C., Scofield, S., Healy, J.M.S., Jacqmard, A., Kilby, N.J., and Murray, J.A.H. (2003). Altered cell cycle distribution, hyperplasia, and inhibited differentiation in Arabidopsis caused by the D-type cyclin CYCD3. Plant Cell **15,** 79–92.

Dharmasiri, N., Dharmasiri, S., and Estelle, M. (2005a). The F-box protein TIR1 is an auxin receptor. Nature **435,** 441–445.

Dharmasiri, N., Dharmasiri, S., Weijers, D., Lechner, E., Yamada, M., Hobbie, L., Ehrismann, J.S., Jürgens, G., and Estelle, M. (2005b). Plant development is regulated by a family of auxin receptor F box proteins. Dev. Cell **9,** 109–119.

Dharmasiri, N., and Estelle, M. (2004). Auxin signaling and regulated protein degradation. Trends Plant Sci. **9,** 302–308.

DiDonato, R.J., Arbuckle, E., Buker, S., Sheets, J., Tobar, J., Totong, R., Grisafi, P., Fink, G.R., and Celenza, J.L. (2004). *Arabidopsis ALF4* encodes a nuclear-localized protein required for lateral root formation. Plant J. **37,** 340–353.

Edlund, A., Eklöf, S., Sundberg, B., Moritz, T., and Sandberg, G. (1995). A microscale technique for gas chromatography-mass spectrometry measurements of picogram amounts of indole-3-acetic acid in plant tissues. Plant Physiol. **108,** 1043–1047.

Eisen, M.B., Spellman, P.T., Brown, P.O., and Botstein, D. (1998). Cluster analysis and display of genome-wide expression patterns. Proc. Natl. Acad. Sci. USA **95,** 14863–14868.

Elledge, S.J., Zhou, Z., Allen, J.B., and Navas, T.A. (1993). DNA damage and cell cycle regulation of ribonucleotide reductase. Bioessays **15,** 333–339.

Friml, J., et al. (2004). A PINOID-dependent binary switch in apical-basal PIN polar targeting directs auxin efflux. Science **306,** 862–865.

Fukaki, H., Nakao, Y., Okushima, Y., Theologis, A., and Tasaka, M. (2005). Tissue-specific expression of stabilized SOLITARY-ROOT/IAA14 alters lateral root development in Arabidopsis. Plant J. **44,** 382–395.

Fukaki, H., Tameda, S., Masuda, H., and Tasaka, M. (2002). Lateral root formation in blocked by a gain-of-function mutation in the *SOLITARY-ROOT/IAA14* gene of *Arabidopsis.* Plant J. **29,** 153–168.

Gautheret, R. (1939). Sur la possibilité de réaliser la culture indéfinie des tissus de tubercule de carotte. C. R. Acad. Sci. **208,** 118–120.

Geldner, N., Richter, S., Vieten, A., Marquardt, S., Torres-Ruiz, R.A., Mayer, U., and Jürgens, G. (2004). Partial loss-of-function alleles reveal a role for *GNOM* in auxin transport-related, post-embryonic development of *Arabidopsis.* Development **131,** 389–400.

Gray, W.M., Kepinski, S., Rouse, D., Leyser, O., and Estelle, M. (2001). Auxin regulates SCF^{TIR1}-dependent degradation of AUX/IAA proteins. Nature **414,** 271–276.

Haecker, A., Groß-Hardt, R., Geiges, B., Sarkar, A., Breuninger, H., Herrmann, M., and Laux, T. (2004). Expression dynamics of *WOX* genes mark cell fate decisions during early embryonic patterning in *Arabidopsis thaliana.* Development **131,** 657–668.

Hagen, G., Martin, G., Li, Y., and Guilfoyle, T.J. (1991). Auxin-induced expression of the soybean GH3 promoter in transgenic tobacco plants. Plant Mol. Biol. **17,** 567–579. Erratum. Plant Mol. Biol. **18,** 1035.

Hemerly, A.S., Ferreira, P., de Almeida Engler, J., Van Montagu, M., Engler, G., and Inzé, D. (1993). *cdc2a* expression in Arabidopsis is linked with competence for cell division. Plant Cell **5,** 1711–1723.

Hennig, L., Menges, M., Murray, J.A.H., and Gruissem, W. (2003). *Arabidopsis* transcript profiling on Affymetrix GeneChip arrays. Plant Mol. Biol. **53,** 457–465.

Hershko, A., and Ciechanover, A. (1998). The ubiquitin system. Annu. Rev. Biochem. **67,** 425–479.

Himanen, K., Boucheron, E., Vanneste, S., de Almeida Engler, J., Inzé, D., and Beeckman, T. (2002). Auxin-mediated cell cycle activation during early lateral root initiation. Plant Cell **14,** 2339–2351.

Himanen, K., Vuylsteke, M., Vanneste, S., Vercruysse, S., Boucheron, E., Alard, P., Chriqui, D., Van Montagu, M., Inzé, D., and Beeckman, T. (2004). Transcript profiling of early lateral root initiation. Proc. Natl. Acad. Sci. USA **101,** 5146–5151.

Hosack, D.A., Dennis, G. Jr, Sherman, B.T., Lane, H.C., and Lempicki, R.A. (2003). Identifying biological themes within lists of genes with EASE. Genome Biol. **4,** R70.1–R70.8.

Hübscher, U., Maga, G., and Spadari, S. (2002). Eukaryotic DNA polymerases. Annu. Rev. Biochem. **71,** 133–163.

Inzé, D. (2005). Green light for the cell cycle. EMBO J. **24,** 657–662.

Ito, T., Kim, G.-T., and Shinozaki, K. (2000). Disruption of an *Arabidopsis* cytoplasmic ribosomal protein S13-homologous gene by transposon-mediated mutagenesis causes aberrant growth and development. Plant J. **22,** 257–264.

Jackson, R.G., Kowalczyk, M., Li, Y., Higgins, G., Ross, J., Sandberg, G., and Bowles, D.J. (2002). Over-expression of an *Arabidopsis* gene encoding a glucosyltransferase of indole-3-acetic acid: Phenotypic characterisation of transgenic lines. Plant J. **32,** 573–583.

Kepinski, S., and Leyser, O. (2005). The *Arabidopsis* F-box protein TIR1 is an auxin receptor. Nature **435,** 446–451.

Kowalczyk, M., and Sandberg, G. (2001). Quantitative analysis of indole-3-acetic acid metabolites in Arabidopsis. Plant Physiol. **127,** 1845–1853.

Kurup, S., Runions, J., Köhler, U., Laplaze, L., Hodge, S., and Haseloff, J. (2005). Marking cell lineages in living tissues. Plant J. **42,** 444–453.

Laskowski, M.J., Williams, M.E., Nusbaum, H.C., and Sussex, I.M. (1995). Formation of lateral root meristems is a two-stage process. Development **121,** 3303–3310.

Lasswell, J., Rogg, L.E., Nelson, D.C., Rongey, C., and Bartel, B. (2000). Cloning and characterization of *IAR1*, a gene required for auxin conjugate sensitivity in Arabidopsis. Plant Cell **12,** 2395–2408.

Lee, J., Das, A., Yamaguchi, M., Hashimoto, J., Tsutsumi, N., Uchimiya, H., and Umeda, M. (2003). Cell cycle function of a rice B2-type cyclin interacting with a B-type cyclin-dependent kinase. Plant J. **34,** 417–425.

Lin, R., and Wang, H. (2005). Two homologous ATP-binding cassette transporter proteins, AtMDR1 and AtPGP1, regulate Arabidopsis photomorphogenesis and root development by mediating polar auxin transport. Plant Physiol. **138,** 949–964.

Liscum, E., and Reed, J.W. (2002). Genetics of Aux/IAA and ARF action in plant growth and development. Plant Mol. Biol. **49,** 387–400.

Liu, W.-m., Mei, R., Di, X., Ryder, T.B., Hubbell, E., Dee, S., Webster, T.A., Harrington, C.A., Ho, M.-h., Baid, J., and Smeekens, S.P. (2002). Analysis of high density expression microarrays with signed-rank call algorithms. Bioinformatics **18,** 1593–1599.

Ljung, K., Hull, A.K., Celenza, J., Yamada, M., Estelle, M., Normanly, J., and Sandberg, G. (2005). Sites and regulation of auxin biosynthesis in Arabidopsis roots. Plant Cell **17,** 1090–1104.

Malamy, J.E., and Benfey, P.N. (1997). Organization and cell differentiation in lateral roots of *Arabidopsis thaliana.* Development **124,** 33–44.

Menges, M., de Jager, S.M., Gruissem, W., and Murray, J.A.H. (2005). Global analysis of the core cell cycle regulators of Arabidopsis identifies novel genes, reveals multiple and highly specific profiles of expression and provides a coherent model for plant cell cycle control. Plant J. **41,** 546–566.

Menges, M., and Murray, J.A.H. (2002). Synchronous *Arabidopsis* suspension cultures for analysis of cell-cycle gene activity. Plant J. **30,** 203–212.

Okushima, Y., et al. (2005). Functional genomic analysis of the *AUXIN RESPONSE FACTOR* gene family members in *Arabidopsis thaliana*: Unique and overlapping functions of *ARF7* and *ARF19.* Plant Cell **17,** 444–463.

Osteryoung, K.W., Stokes, K.D., Rutherford, S.M., Percival, A.L., and Lee, W.Y. (1998). Chloroplast division in higher plants requires members of two functionally divergent gene families with homology to bacterial *ftsZ.* Plant Cell **10,** 1991–2004.

Ouellet, F., Overvoorde, P.J., and Theologis, A. (2001). IAA17/AXR3: Biochemical insight into an auxin mutant phenotype. Plant Cell **13,** 829–841.

Paponov, I.A., Teale, W.D., Trebar, M., Blilou, I., and Palme, K. (2005). The PIN auxin efflux facilitators: Evolutionary and functional perspectives. Trends Plant Sci. **10,** 170–177.

Park, J.-Y., Kim, H.-J., and Kim, J. (2002). Mutation in domain II of IAA1 confers diverse auxin-related phenotypes and represses auxin-activated expression of *Aux/IAA* genes in steroid regulator-inducible system. Plant J. **32,** 669–683.

Parry, G., et al. (2001). Quick on the uptake: Characterization of a family of plant auxin influx carriers. J. Plant Growth Regul. **20,** 217–225.

Porceddu, A., Stals, H., Reichheld, J.-P., Segers, G., De Veylder, L., De Pinho Barrôco, R., Casteels, P., Van Montagu, M., Inzé, D., and Mironov, V. (2001). A plant-specific cyclin-dependent kinase is involved in the control of G_2/M progression in plants. J. Biol. Chem. **276,** 36354–36360.

Puthoff, D.P., Nettleton, D., Rodermel, S.R., and Baum, T.J. (2003). Arabidopsis gene expression changes during cyst nematode parasitism revealed by statistical analyses of microarray expression profiles. Plant J. **33,** 911–921.

Ramos, J.A., Zenser, N., Leyser, O., and Callis, J. (2001). Rapid degradation of auxin/indoleacetic acid proteins requires conserved amino acids of domain II and is proteasome dependent. Plant Cell **13,** 2349–2360.

Rampey, R.A., LeClere, S., Kowalczyk, M., Ljung, K., Sandberg, G., and Bartel, B. (2004). A family of auxin-conjugate hydrolases that contributes to free indole-3-acetic acid levels during Arabidopsis germination. Plant Physiol. **135,** 978–988.

Roudier, F., Fedorova, E., Györgyey, J., Feher, A., Brown, S., Kondorosi, A., and Kondorosi, E. (2000). Cell cycle function of a *Medicago sativa* A2-type cyclin interacting with a PSTAIRE-type cyclin-dependent kinase and a retinoblastoma protein. Plant J. **23,** 73–83.

Sabatini, S., Beis, D., Wolkenfelt, H., Murfett, J., Guilfoyle, T., Malamy, J., Benfey, P., Leyser, O., Bechtold, N., Weisbeek, P., and Scheres, B. (1999). An auxin-dependent distal organizer of pattern and polarity in the *Arabidopsis* root. Cell **99,** 463–472.

Sachs, T. (1988). Epigenetic selection: An alternative mechanism of pattern formation. J. Theor. Biol. **134,** 547–559.

Saeed, A.I., et al. (2003). TM4: A free, open-source system for microarray data management and analysis. Biotechniques **34,** 374–378.

Schrader, J., Baba, K., May, S.T., Palme, K., Bennett, M., Bhalerao, R.P., and Sandberg, G. (2003). Polar auxin transport in the wood-forming tissues of hybrid aspen is under simultaneous control of developmental and environmental signals. Proc. Natl. Acad. Sci. USA **100,** 10096–10101.

Shimotohno, A., Umeda-Hara, C., Bisova, K., Uchimiya, H., and Umeda, M. (2004). The plant-specific kinase CDKF;1 is involved in activating phosphorylation of cyclin-dependent kinase-activating kinases in Arabidopsis. Plant Cell **16,** 2954–2966.

Soukas, A., Cohen, P., Socci, N.D., and Friedman, J.M. (2000). Leptin-specific patterns of gene expression in white adipose tissue. Genes Dev. **14,** 963–980.

Staswick, P.E., Serban, B., Rowe, M., Tiryaki, I., Maldonado, M.T., Maldonado, M.C., and Suza, W. (2005). Characterization of an Arabidopsis enzyme family that conjugates amino acids to indole-3-acetic acid. Plant Cell **17,** 616–627.

Staswick, P.E., Tiryaki, I., and Rowe, M.L. (2002). Jasmonate response locus *JAR1* and several related Arabidopsis genes encode enzymes of the firefly luciferase superfamily that show activity on jasmonic, salicylic, and indole-3-acetic acids in an assay for adenylation. Plant Cell **14,** 1405–1415.

Stevens, R., Mariconti, L., Rossignol, P., Perennes, C., Cella, R., and Bergounioux, C. (2002). Two E2F sites in the *Arabidopsis MCM3* promoter have different roles in cell cycle activation and meristematic expression. J. Biol. Chem. **277,** 32978–32984.

Storey, J.D., and Tibshirani, R. (2003). Statistical significance for genomewide studies. Proc. Natl. Acad. Sci. USA **100,** 9440–9445.

Sun, Y., Dilkes, B.P., Zhang, C., Dante, R.A., Carneiro, N.P., Lowe, K.S., Jung, R., Gordon-Kamm, W.J., and Larkins, B.A. (1999). Characterization of maize (*Zea mays* L.) Wee1 and its activity in developing endosperm. Proc. Natl. Acad. Sci. USA **96,** 4180–4185.

Taji, T., Seki, M., Satou, M., Sakurai, T., Kobayashi, M., Ishiyama, K., Narusaka, Y., Narusaka, M., Zhu, J.-K., and Shinozaki, K. (2004). Comparative genomics in salt tolerance between Arabidopsis and Arabidopsis-related halophyte salt cress using Arabidopsis microarray. Plant Physiol. **135,** 1697–1709.

Tavazoie, S., Hughes, J.D., Campbell, M.J., Cho, R.J., and Church, G.M. (1999). Systematic determination of genetic network architecture. Nat. Genet. **22,** 281–285.

Tian, C.E., Muto, H., Higuchi, K., Matamura, T., Tatematsu, K., Koshiba, T., and Yamamoto, K.T. (2004). Disruption and overexpression of auxin response factor 8 gene of Arabidopsis affect hypocotyl elongation and root growth habit, indicating its possible involvement in auxin homeostasis in light condition. Plant J. **40,** 333–343.

Tian, Q., Uhlir, N.J., and Reed, J.W. (2002). Arabidopsis SHY2/IAA3 inhibits auxin-regulated gene expression. Plant Cell **14,** 301–319.

Tiwari, S.B., Hagen, G., and Guilfoyle, T.J. (2004). Aux/IAA proteins contain a potent transcriptional repression domain. Plant Cell **16,** 533–543.

Torrey, J.G. (1950). The induction of lateral roots by indoleacetic acid and root decapitation. Am. J. Bot. **37,** 257–264.

Ullah, H., Chen, J.-G., Temple, B., Boyes, D.C., Alonso, J.M., Davis, K.R., Ecker, J.R., and Jones, A.M. (2003). The β-subunit of the Arabidopsis G protein negatively regulates auxin-induced cell division and affects multiple developmental processes. Plant Cell **15,** 393–409.

Ulmasov, T., Murfett, J., Hagen, G., and Guilfoyle, T.J. (1997). Aux/IAA proteins repress expression of reporter genes containing natural and highly active synthetic auxin response elements. Plant Cell **9,** 1963–1971.

Vandepoele, K., Raes, J., De Veylder, L., Rouzé, P., Rombauts, S., and Inzé, D. (2002). Genome-wide analysis of core cell cycle genes in Arabidopsis. Plant Cell **14,** 903–916.

Van Lijsebettens, M., Vanderhaeghen, R., De Block, M., Bauw, G., Villarroel, R., and Van Montagu, M. (1994). An S18 ribosomal protein gene copy, encoded at the *Arabidopsis PFL* locus, affects plant development by its specific expression in meristems. EMBO J. **13,** 3378–3388.

Vanneste, S., Maes, L., De Smet, I., Himanen, K., Naudts, M., Inzé, D., and Beeckman, T. (2005). Auxin regulation of cell cycle and its role during lateral root initiation. Physiol. Plant. **123,** 139–146.

Vieten, A., Vanneste, S., Wiśniewska, J., Benková, E., Benjamins, R., Beeckman, T., Luschnig, C., and Friml, J. (2005). Functional redundancy of PIN proteins is accompanied by auxin-dependent cross-regulation of PIN expression. Development **132,** 4521–4531.

Wang, H., Fowke, L.C., and Crosby, W.L. (1997). A plant cyclin-dependent kinase inhibitor gene. Nature **386,** 451–452.

Weijers, D., and Jürgens, G. (2004). Funneling auxin action: Specificity in signal transduction. Curr. Opin. Plant Biol. **7,** 687–693.

Wilmoth, J.C., Wang, S., Tiwari, S.B., Joshi, A.D., Hagen, G., Guilfoyle, T.J., Alonso, J.M., Ecker, J.R., and Reed, J.W. (2005). NPH4/ARF7 and ARF19 promote leaf expansion and auxin-induced lateral root formation. Plant J. **43,** 118–130.

Yeung, K.Y., Haynor, D.R., and Ruzzo, W.L. (2001). Validating clustering for gene expression data. Bioinformatics **17,** 309–318.

Zenser, N., Ellsmore, A., Leasure, C., and Callis, J. (2001). Auxin modulates the degradation rate of Aux/IAA proteins. Proc. Natl. Acad. Sci. USA **98,** 11795–11800.

Zhao, Y., Christensen, S.K., Fankhauser, X., Cashman, J.R., Cohen, J.D., Weigel, D., and Chory, J. (2001). A role for flavin monooxygenase-like enzymes in auxin biosynthesis. Science **291,** 306–309.

Zhao, Y., Hull, A.K., Gupta, N.R., Goss, K.A., Alonso, J., Ecker, J.R., Normanly, J., Chory, J., and Celenza, J.L. (2002). Trp-dependent auxin biosynthesis in *Arabidopsis*: Involvement of cytochrome P450s CYP79B2 and CYP79B3. Genes Dev. **16,** 3100–3112.

Zimmermann, P., Hirsch-Hoffmann, M., Hennig, L., and Gruissem, W. (2004). GENEVESTIGATOR. Arabidopsis microarray database and analysis toolbox. Plant Physiol. **136,** 2621–2632.